

Molecular Recognition by Cholesterol Esterase of Active Site Ligands: Structure–Reactivity Effects for Inhibition by Aryl Carbamates and Subsequent Carbamylenzyme Turnover[†]

Shawn R. Feaster,[‡] Keun Lee,[‡] Nathan Baker,[‡] David Y. Hui,[§] and Daniel M. Quinn^{*,‡}

Department of Chemistry, The University of Iowa, Iowa City, Iowa 52242, and Department of Pathology, University of Cincinnati College of Medicine, Cincinnati, Ohio 45267

Received July 10, 1996; Revised Manuscript Received October 22, 1996[®]

ABSTRACT: Interactions of mammalian pancreatic cholesterol esterases from pig and rat with a family of aryl carbamates $C_nH_{2n+1}NHCOOAr$ [$n = 4–9$; $Ar = \text{phenyl, } p\text{-X-phenyl (X = acetamido, bromo, fluoro, nitro, trifluoromethyl), 2-naphthyl, 2-tetrahydronaphthyl, estronyl}$] have been investigated, with an aim of delineating the ligand structural features which lead to effective molecular recognition by the active site of the enzyme. These carbamates inhibit the catalytic activity of CEase by rapid carbamylation of the active site, a process that shows saturation kinetics. Subsequent slow decarbamylation usually leads to full restoration of activity, and therefore aryl carbamates are transient inhibitors, or pseudo-substrates, of CEase. Structural variation of carbamate inhibitors allowed molecular recognition in the fatty acid binding and steroid binding loci of the extended active site to be probed, and the electronic nature of the carbamylation transition state to be characterized. Optimal inhibitory activity is observed when the length of the carbamyl function is $n = 6$ and $n = 7$ for porcine and rat cholesterol esterases, respectively, equivalent to eight- and nine-carbon fatty acyl chains. In contrast, inhibitory activity increases progressively as the partial molecular volume of the aromatic fragment increases. Hammett plots for p -substituted phenyl- N -hexyl carbamates indicate that the rate-determining step for carbamate inhibition is phenolate anion expulsion. Effects of the bile salt activator taurocholate on the kinetically resolved phases of the pseudo-substrate turnover of aryl carbamates were also studied. Taurocholate increases the affinity of the carbamate for the active site of cholesterol esterase in the reversible, noncovalent complex that precedes carbamylation and increases the rate constants of the serial carbamylation and decarbamylation steps. Structural variation of the N -alkyl chain and of the aryl fused-ring system provides an accounting of bile salt modulation of the fatty acid and steroid binding sites, respectively. In that pseudo-substrate turnover of aryl carbamates proceeds by a three-step mechanism that is analogous to that for rapid turnover of lipid ester substrates, these investigations illuminate details of ligand recognition by the extended active site of cholesterol esterase that are prominent determinants of the substrate specificity and catalytic power of the enzyme.

Mammalian pancreatic cholesterol esterase (CEase;¹ cholesteryl ester hydrolase, EC 3.1.1.13) is a lipolytic enzyme that has a broad substrate specificity. CEase catalyzes the hydrolysis of a wide range of ester substrates, including cholesteryl esters, acylglycerides, phospholipids (Brockerhoff & Jensen, 1974; Kritchevsky & Kothari, 1978; Rudd & Brockman, 1984), retinyl esters (Fredrikzon *et al.*, 1978), vitamin esters (Rudd & Brockman, 1984), and phenyl esters (Rudd & Brockman, 1984), and the enzyme has even been

demonstrated to have amidase activity (Hui *et al.*, 1993). Of the pancreatic lipolytic enzymes that are secreted into the duodenum in response to an alimentary load, CEase alone has high hydrolytic activity on cholesteryl esters. In a water-limited environment, CEase catalyzes transacylation reactions, such as cholesteryl ester synthesis (Gallo *et al.*, 1977) and alcoholysis, a feature that makes the enzyme a useful biocatalyst (Kazlauskas, 1989). Despite the broad specificity and synthetic utility of the enzyme, our understanding is limited of the nature of the interactions between substrates and the CEase active site that lead to effective catalysis.

CEase belongs to the α/β hydrolase fold family of proteins (Ollis *et al.*, 1992; Cygler *et al.*, 1993) whose members share secondary and tertiary structural features. Most of the members of this family are esterases, and nearly all of these utilize a serine esterase catalytic mechanism, outlined in Scheme 1, that is reminiscent of the serine protease mechanism (Kraut, 1977). Like the serine proteases, CEase possesses a triad, Ser194-His435-Asp320, that serves as a nucleophilic and general acid–base catalytic entity. These assignments have been supported by site-directed mutagenesis experiments (DiPersio *et al.*, 1990, 1991; DiPersio & Hui, 1993), by the effects of irreversible inhibitors (Abouakil

[†] Supported by American Heart Association Grant-In-Aid 91-15220 to D.M.Q. and NIH Grant R01 DK40917 to D.Y.H. S.R.F. was supported by a Predoctoral Training Program in Biotechnology, NIH Grant 1T32 GM08365.

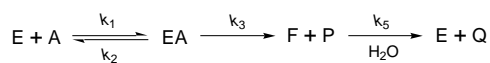
[‡] Department of Chemistry, The University of Iowa.

[§] Department of Pathology, University of Cincinnati College of Medicine.

* Address correspondence to this author. Tel: (319) 335-1335. FAX: (319) 335-1270. E-mail: daniel-quinn@uiowa.edu.

[®] Abstract published in *Advance ACS Abstracts*, December 1, 1996.

¹ Abbreviations: CEase, cholesterol esterase; EDTA, ethylenediamine tetraacetic acid; PCEase, porcine CEase; PNPB, p -nitrophenyl butyrate; RCEase, rat CEase; NaTC, sodium taurocholate; SAR, structure–activity relationship; TLC, thin-layer chromatography; THF, tetrahydrofuran. Amino acid abbreviations: Asp, aspartate, His, histidine, Ser, serine, Pro, proline, Ala, alanine, Glu, glutamate, Leu, leucine, Met, methionine, Trp, tryptophan, Tyr, tyrosine, Val, valine, and Phe, phenylalanine.

Scheme 1: Acylenzyme^a and Carbamylenzyme^b Mechanisms

^a Ester hydrolysis: A = ester; EA = Michaelis complex; F = acylenzyme; P, Q = respective alcohol and acid products; k_3 , k_5 = respective acylation and deacylation rate constants. ^b Carbamate inhibition: A = carbamate; EA = noncovalent complex; F = carbamylenzyme; P, Q = respective phenol and carbamic acid products; k_3 , k_5 = respective carbamylation and decarbamylation rate constants.

et al., 1989; DiPersio *et al.*, 1990; Baba *et al.*, 1991), and by nucleophilic trapping experiments (Lombardo & Guy, 1981; Stout *et al.*, 1985; Sutton *et al.*, 1990a).

In the investigations described herein, the aryl carbamates whose structures are shown in Table 1 were synthesized and evaluated as inhibitors of porcine and rat pancreatic CEases. The range of inhibitor structures was chosen to probe the electronic nature of the carbamylation transition state and to provide structure–activity probes of two loci that converge at Ser194 of the active site triad that are important determinants of molecular recognition of cholesteryl esters. Variation of the *N*-alkyl chain length probes the saturated fatty acyl specificity of CEase; progressive elaboration of the aryl portion from a single ring to an aromatic steroid probes the steroid ring binding locus of the enzyme. Furthermore, the resolution of the carbamylenzyme mechanism into the three stages outlined in Scheme 1 allows structure–activity relationships (SARs) to be developed for each stage. These SARs are interpreted, with the aid of a recently developed molecular model of CEase, in terms of the structural elements of CEase that underlie the cholesteryl ester hydrolytic specificity of the enzyme.

MATERIALS AND METHODS

Materials. PNPB and TX100 were purchased from Sigma Chemical Co. The following reagents were purchased from Aldrich Chemical Co.: *p*-X-phenols (X = acetamido, bromo, fluoro, nitro, trifluoromethyl), 2-naphthol, estrone, 5,6,7,8-tetrahydro-2-naphthol, hexanoyl chloride, heptanoyl chloride, octanoyl chloride, *n*-butyl isocyanate, triethylamine, and sodium azide. *n*-Octyl isocyanate and *n*-hexyl isocyanate were purchased from Eastman-Kodak. Silica gel (230–400 mesh) and HPLC-grade hexane and ethyl acetate were purchased from EM Science. TLC plates (polygram sil G/UV254, silica gel with fluorescent indicator) were purchased from Brinkman Instruments, Inc. Water for buffer preparation was distilled and then deionized by passage through a mixed bed ion-exchange column (Barnsted, Sybron Corp.). Organic solvents were distilled prior to use. Buffer salts were commercially available reagent-grade materials.

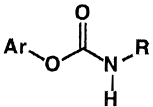
Enzyme Purification. Porcine CEase (PCEase) was purified as previously described (Sutton *et al.*, 1990a). Rat CEase (RCEase) was purified by the following procedure: First, 22 g of Sprague-Dawley rat pancreata were homogenized at pH 6.30 and 5 °C in 100 mL of 0.5% digitonin solution containing 1 mM EDTA, 0.02% NaN₃, and 0.154 M NaCl. The homogenate was thoroughly mixed in an ice-water bath for 30 min followed by filtration through glass wool. The resulting filtrate was centrifuged at 105000g for 45 min at 5 °C. The proteins were then salted out of the supernatants by adding 288 mg mL⁻¹ of ammonium sulfate followed by constant stirring for 15 min at <4 °C. The proteins were pelleted by centrifugation at 15000g for 45






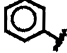
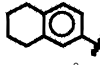
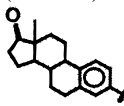
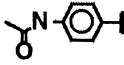
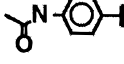
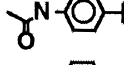
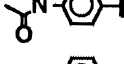
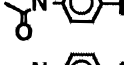
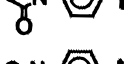
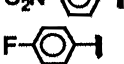
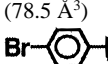
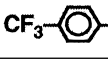
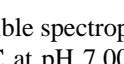
min at 5 °C. The proteins were resuspended in a minimum volume of 0.01 M sodium phosphate buffer containing 0.1 M NaCl, 1 mM EDTA, 0.02% NaN₃, and 1.5% glycerol at pH 6.30 before being applied to a 440 mL Sephacryl S200HR column. The proteins were fractionated on the S200HR matrix using 0.01 M sodium phosphate buffer containing 0.1 M NaCl, 1 mM EDTA, 0.02% NaN₃, 1.5% glycerol at pH 6.30 and a flow rate of 120 mL h⁻¹. Fractions from the column possessing the highest catalytic activity, based on PNPB hydrolysis, and highest A₂₈₀ values were pooled together and applied to a 40 mL Affi-Gel Blue column (Bio-Rad). The unbound proteins were eluted from the column at a flow rate of 30 mL h⁻¹ using 0.01 M sodium phosphate buffer containing 0.1 M NaCl, 1 mM EDTA, 0.02% NaN₃, 1.5% glycerol at pH 6.30. Once all of the unbound proteins were eliminated from the Affi-Gel Blue matrix, the bound RCEase was eluted from the column at a flow rate of 30 mL h⁻¹ using a linear salt gradient (0.154–1.5 M NaCl) in the aforementioned buffer system. The fractions containing the greatest catalytic activity and A₂₈₀ values were pooled together. Next, the protein was salted out of solution using 288 mg mL⁻¹ (NH₄)₂SO₄ described earlier. Finally, the protein was resuspended in a minimum volume of 0.01 M sodium phosphate buffer containing 0.1 M NaCl, 1 mM EDTA, 0.02% NaN₃, and 1.5% glycerol at pH 6.30. The solution was then applied to a 25 mL sephadex G25 column for desalting.

Aryl Carbamate Synthesis. The following procedure for synthesis of 2-naphthyl-*N*-heptyl carbamate exemplifies the synthetic methods that were used to produce the carbamates shown in Table 1. *N*-Heptyl isocyanate was synthesized by the Curtius rearrangement of octanoyl azide. Sodium azide (9.75 g, 15 mmol) in 60 mL of distilled water and 60 mL of cyclohexane was cooled in an ice bath and stirred until completely dissolved. Octanoyl chloride (16.2 g, 10 mmol) in 50 mL of acetone was added dropwise to the solution while keeping the temperature below 15 °C. The resulting solution was stirred vigorously for 3 h at ~10 °C, and the organic layer was separated in a separatory funnel. This octanoyl azide solution was added dropwise to boiling cyclohexane (50 mL) at a rate that maintained the temperature above 65 °C, and the resulting solution was stirred for 3 h at 65–70 °C. After removal of excess solvent by rotary evaporation, ~30 mL of concentrated heptyl isocyanate solution remained in the flask. To a solution of 2-naphthol (3 g, 20 mmol) in 70 mL of THF, 10 mL (~60 mmol) of heptyl isocyanate solution was added dropwise, followed by 0.4 mL of triethylamine, and the solution was stirred overnight at room temperature. Completeness of reaction was verified by the absence of a spot for the 2-naphthol reactant on TLC in 8:3 (v/v) ethylacetate:hexane. THF and excess heptyl isocyanate were removed by rotary evaporation and the resulting solid was recrystallized twice from petroleum ether and acetone. The crystalline product gave a single spot at *R*_f = 0.77 on TLC in the above solvent system and melted sharply at 101–102 °C. ¹H-NMR (recorded at 360 MHz on a Bruker WM360 spectrometer), mass spectra (recorded on a VG-TRIO1), and C/H/N elemental analysis were consistent with the expected structure and lack of detectable contamination of the carbamate.

Because the appropriate isocyanates were commercially available, the Curtius rearrangement step was unnecessary for syntheses of *N*-butyl, *N*-hexyl, and *N*-octyl carbamates.

Table 1: Fragment Volumes and Hammet Substituent Constants for Aryl-*N*-alkyl Carbamates



compound	compound name	Ar (volume)	R (volume)	σ_p^-
1	2-naphthyl- <i>N</i> -butyl carbamate	 (113.4 Å ³)	<i>n</i> -butyl (78.6 Å ³)	NA
2	2-naphthyl- <i>N</i> -pentyl carbamate	 (113.4 Å ³)	<i>n</i> -pentyl (95.2 Å ³)	NA
3	2-naphthyl- <i>N</i> -hexyl carbamate	 (113.4 Å ³)	<i>n</i> -hexyl (111.9 Å ³)	NA
4	2-naphthyl- <i>N</i> -heptyl carbamate	 (113.4 Å ³)	<i>n</i> -heptyl (128.0 Å ³)	NA
5	2-naphthyl- <i>N</i> -octyl carbamate	 (113.4 Å ³)	<i>n</i> -octyl (144.1 Å ³)	NA
6	phenyl- <i>N</i> -hexyl carbamate	 (74.7 Å ³)	<i>n</i> -hexyl	NA
7	2-(5,6,7,8-tetrahydronaphthyl)- <i>N</i> -hexyl carbamate	 (129.6 Å ³)	<i>n</i> -hexyl	NA
8	2-estranyl- <i>N</i> -hexyl carbamate	 (227.0 Å ³)	<i>n</i> -hexyl	NA
9	<i>p</i> -acetamido- <i>N</i> -butyl carbamate	 (129.6 Å ³)	<i>n</i> -butyl	NA
10	<i>p</i> -acetamido- <i>N</i> -pentyl carbamate	 (129.6 Å ³)	<i>n</i> -pentyl	NA
11	<i>p</i> -acetamido- <i>N</i> -hexyl carbamate	 (129.6 Å ³)	<i>n</i> -hexyl	−0.46
12	<i>p</i> -acetamido- <i>N</i> -heptyl carbamate	 (129.6 Å ³)	<i>n</i> -heptyl	NA
13	<i>p</i> -acetamido- <i>N</i> -octyl carbamate	 (129.6 Å ³)	<i>n</i> -octyl	NA
14	<i>p</i> -acetamido- <i>N</i> -nonyl carbamate	 (129.6 Å ³)	<i>n</i> -nonyl (160.2 Å ³)	NA
15	<i>p</i> -nitrophenyl- <i>N</i> -hexyl carbamate	 (129.6 Å ³)	<i>n</i> -hexyl	1.24
16	<i>p</i> -fluorophenyl- <i>N</i> -hexyl carbamate	 (78.5 Å ³)	<i>n</i> -hexyl	0.05
17	<i>p</i> -bromophenyl- <i>N</i> -hexyl carbamate	 (78.5 Å ³)	<i>n</i> -hexyl	0.28
18	<i>p</i> -(trifluoromethyl)phenyl- <i>N</i> -hexyl carbamate	 (78.5 Å ³)	<i>n</i> -hexyl	0.65

Noncrystalline carbamates (e.g., phenyl-*N*-hexyl carbamate) were purified by reversed-phase HPLC using a Dynamix-60A (Rainin Instrument Company, Inc.) preparative axial compression C₁₈ column (41.4 mm × 25 cm, 8 μ particle size). The mixture was fractionated using a linear gradient (50–70% v/v) of acetonitrile in water at a flow rate of 10 mL min^{−1}. The fraction corresponding to 59.7–60.8% acetonitrile:water contained the desired carbamates.

Enzyme Kinetics. CEase activity was measured by following the hydrolysis of the colorimetric substrate *p*-nitrophenyl butyrate (PNPB) at 400 nm on an HP8452A

UV–visible spectrophotometer. Reactions were run at 25.0 ± 0.2 °C at pH 7.00 (RCEase) or 7.04 (PCEase) in 0.1 M sodium phosphate buffers that contained 0.16 M NaCl (RCEase) or 0.1 M NaCl (PCEase). The Michaelis constant *K_m* for this reaction was determined by measuring initial velocity *v* as a function of substrate concentration [A] and fitting the resulting data to the Michaelis–Menten equation:

$$v = \frac{V_{\max}[A]}{K_m + [A]} \quad (1)$$

Except where indicated, all data analyses described herein utilized nonlinear least-squares procedures (Wentworth, 1964) and computer programs that were written in the laboratory of the corresponding author.

Calculation of Molecular Fragment Volumes. Fragment volumes that are used in structure–activity correlations were calculated via molecular modeling on a Silicon Graphics XS24 workstation using the commercial software package Sybyl 6.10 (Tripos, Inc.). The following procedure was used. First, the appropriate fragment was sketched using standard molecular modeling techniques. The *N*-alkyl chains were sketched in the *trans-anti-trans* configuration starting with the amide nitrogen (*NB*: the nitrogen was fully protonated). The phenol moieties were generated from benzene or naphthalene, standard Sybyl library fragments. Second, the fragments were minimized via molecular mechanics to an energy gradient cutoff of 0.05 kcal mol⁻¹ Å⁻¹. Each minimization utilized the Tripos force field, Gasteiger–Hückel electrostatic charge calculations, and the remaining parameters were set at their default values. Next, the phenol or amine proton was removed from the fragment. Finally, the volume for each fragment was calculated from the corresponding Connolly surface generated by using the MOLCAD module in Sybyl, with all values set at their defaults.

RESULTS

Characterization of Transient Carbamate Inhibition. Aryl carbamates transiently inhibit CEase-catalyzed hydrolysis of PNPB by the mechanism in Scheme 1. The carbamylation stage is rapid compared to subsequent decarbamylation, and thus the two stages are easily resolved kinetically. In the presence of a carbamate inhibitor, time courses for hydrolysis of PNPB are biphasic, as shown in Figure 1A for inhibition of RCEase by 2-naphthyl-*N*-butyl carbamate and described by eq 2:

$$A = A_0 + \frac{v_0 - v_{ss}}{k}(1 - e^{-kt}) + v_{ss}t \quad (2)$$

In eq 1 A_0 , k , v_0 , and v_{ss} are the absorbance at $t = 0$, the observed first-order inhibition rate constant, the initial velocity, and the steady-state velocity, respectively. The nonlinear presteady-state phase monitors progressive loss of enzyme activity, as the time-dependent decrease in slope indicates. In the linear steady-state phase of the reaction, the rates of carbamylation and decarbamylation are equal. The dependence of k on $[I]$, the concentration of the carbamate inhibitor, is given by eq 3:

$$k = \frac{k_3[I]}{K_i + [I]} \quad (3)$$

Figure 1B shows a fit to eq 3 of k versus $[I]$ data for inhibitions of RCEase by 2-naphthyl-*N*-heptyl carbamate. As Scheme 1 shows, k_3 is the rate constant for carbamylation of Ser194. K_i is the apparent dissociation constant of the reversible, noncovalent enzyme–carbamate complex. From this $K_c = k_2/k_1$ is calculated as

$$K_c = \frac{K_i}{1 + [A]/K_m} \quad (4)$$

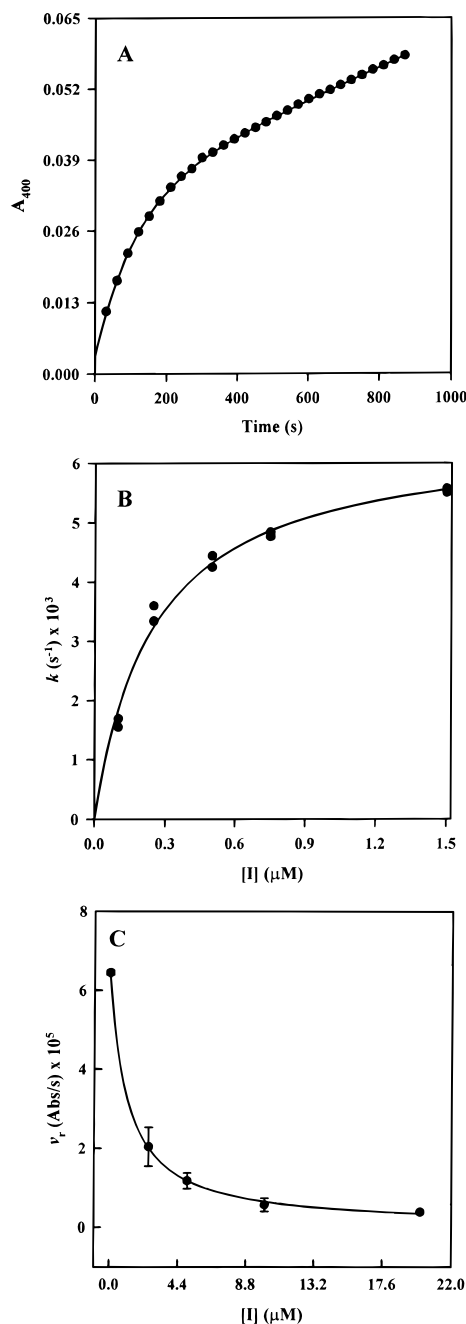


FIGURE 1: Kinetics of arylcarbamate inhibition of RCEase. A. Biphasic time course for inhibition by 2-naphthyl-*N*-butyl carbamate, **1**. The reaction was run as described in Materials and Methods and contained 100 μ M NaTC, 50 μ M PNPB, 5.0 μ M **1**, 2.7 nM RCEase, and 2% acetonitrile (v/v). The solid line is a nonlinear least-squares fit to eq 2; the parameters of the fit are $A_0 = 0.0042 \pm 0.0001$, $k = (9.73 \pm 0.03) \times 10^{-3} \text{ s}^{-1}$, $v_{ss} = (3.157 \pm 0.005) \times 10^{-5} \text{ Å s}^{-1}$, and $v_0 = (3.438 \pm 0.005) \times 10^{-4} \text{ Å s}^{-1}$. B. Nonlinear dependence of k on $[I]$ for inhibition of RCEase by 2-naphthyl-*N*-heptyl carbamate, **4**. The reactions were run as described in Materials and Methods and contained 50 μ M PNPB, 0.10–1.50 μ M **4**, 1.35–2.70 nM RCEase and 2% acetonitrile (v/v). The solid line is a nonlinear least-squares fit to eq 3; the parameters of the fit are $k_3 = (6.5 \pm 0.2) \times 10^{-3} \text{ s}^{-1}$ and $K_i = (2.5 \pm 0.3) \times 10^{-7} \text{ M}$. C. Nonlinear dependence of v_i on $[I]$ for inhibition of RCEase by phenyl-*N*-hexyl carbamate, **6**. The reactions were run as described in Materials and Methods and contained 50 μ M PNPB, 2.5–20 μ M **6**, 15–180 pM RCEase, and 2% acetonitrile (v/v). The solid line is a nonlinear least-squares fit to eq 5; the parameters of the fit are $v_0 = (6.4 \pm 0.1) \times 10^{-5} \text{ Å s}^{-1}$ and $K_d = (1.1 \pm 0.1) \times 10^{-7} \text{ M}$, and v_{min} was set at 0.

The steady-state velocity v_{ss} contains contributions from nonenzymic hydrolysis of PNPB and from turnover of the

Table 2: Dissociation and Kinetic Constants for Inhibition of RCEase by Aryl-*N*-alkyl Carbamates

compound	[NaTC] ^a (mM)	10 ² <i>k</i> ₃ ^b (s ⁻¹)	<i>k</i> ₃ / <i>K</i> _C ^c (M ⁻¹ s ⁻¹)	10 ⁴ <i>k</i> ₅ ^c (s ⁻¹)	<i>K</i> _c ^b (μM)	<i>K</i> _d ^d (nM)
1	0	2.3 ± 0.1	2400 ± 20	1.610 ± 0.003	8.0 ± 0.9	130 ± 30
	5.8	44 ± 3	10500 ± 200	1.456 ± 0.008	7 ± 1	11 ± 3
2	0	1.8 ± 0.1	1140 ± 10	1.433 ± 0.007	4 ± 1	140 ± 20
	5.8	23 ± 1	11300 ± 200	1.243 ± 0.004	3.8 ± 0.6	20 ± 10
3	0	1.68 ± 0.09	6650 ± 70	0.970 ± 0.002	0.9 ± 0.1	18 ± 2
	5.8	41 ± 3	53000 ± 3000	1.708 ± 0.007	1.1 ± 0.2	0.8 ± 0.1
4	0	0.65 ± 0.02	10000 ± 100	0.919 ± 0.003	0.18 ± 0.02	7.3 ± 0.7
	5.8	19.4 ± 0.6	108000 ± 3000	2.833 ± 0.005	0.15 ± 0.02	0.5 ± 0.1
5	0	0.142 ± 0.007	7010 ± 70	0.708 ± 0.001	0.07 ± 0.01	15 ± 1
	5.8	8.3 ± 0.8	88000 ± 2000	2.282 ± 0.003	0.21 ± 0.06	6 ± 1
6	0	0.071 ± 0.006	ND	ND	4 ± 1	800 ± 80
	5.8	6.8 ± 0.4	ND	ND	12 ± 1	52 ± 2
7	0	2.5 ± 0.4	ND	ND	2.2 ± 0.3	20 ± 10
	5.8	27 ± 2	ND	ND	0.38 ± 0.06	16 ± 8
8	0	2.73 ± 0.08	ND	ND	0.283 ± 0.008	2.1 ± 0.4
	5.8	18.2 ± 0.6	ND	ND	0.030 ± 0.003	2.0 ± 0.3

^a Reactions were run at 25.0 ± 0.1 °C in 970 μL of 0.1 M sodium phosphate buffer, pH 7.00, that contained 0.16 M NaCl, 0 or 6.0 mM NaTC, 10 μL of 50 μM PNPB dissolved in HPLC grade acetonitrile, 10 μL of inhibitor dissolved in HPLC grade acetonitrile, and 10 μL of enzyme containing 2 mM TX-100. ND = not determined. ^b Rate constant calculated by nonlinear least-squares fitting of *k* versus [I] data to eq 3. ^c Rate constant calculated by fourth-order Runge–Kutta numerical simulation as described in Results and in Shin and Quinn (1992). ^d Obtained from fitting *V_r* versus [I] data to eq 5.

carbamylenzyme complex, governed by rate constant *k*₅ in Scheme 1. When the nonenzymic rate of PNPB hydrolysis, determined in a control reaction that is devoid of CEase, is subtracted from *v*_{ss}, the resulting residual velocity *v_r* is also a function of [I]:

$$v_r = \frac{v_0(K_d + v_{\min}[I])}{K_d + [I]} \quad (5)$$

Figure 1C shows a fit of *v_r* versus [I] data to eq 5 for inhibition by phenyl-*N*-hexyl carbamate. In eq 5 *v*_{min} = *V_Ak*₅/(*k*₃ + *k*₅), where *V_A* = *V*_{max}[A]/(*K*_m + [A]) for turnover of PNPB in the absence of inhibitor (*i.e.*, control reaction). Therefore *v*_{min}/*V_A* = *k*₅/(*k*₃ + *k*₅); for the carbamylenzyme reactions described herein *k*₅ ≪ *k*₃ and thus *v*_{min}/*V_A* = *k*₅/*k*₃. Since *k*₃ is known from fits to eq 3, *k*₅, the decarbamylation rate constant, can be calculated. The constant *K*_d = *K_Ck*₅/*k*₃ provides a second way to calculate *k*₅, since *K_C* is known from fits to eq 3, as calculated in eq 4. Carbamate inhibition parameters were characterized in the absence and presence of a bile salt activator of CEase, sodium taurocholate. The values so determined for *K_C*, *K*_d, and *k*₃ for the various carbamate inhibitors in Scheme 1 are collected in Table 2.

The decarbamylation rate constant, *k*₅ in Scheme 1, can also be determined by following the full time course for serial carbamylation, steady-state turnover (wherein the rates of carbamylation and decarbamylation are approximately equal), and decarbamylation. In this case, the differential equations for [E], [A], and [F] (cf. Scheme 1) are as follows:

$$\frac{d[E]}{dt} = k_5[F] - \frac{k_3}{K_C}[E][A] \quad (6)$$

$$\frac{d[A]}{dt} = -\frac{k_3}{K_C}[E][A] \quad (7)$$

$$\frac{d[F]}{dt} = \frac{k_3}{K_C}[E][A] - k_5[F] \quad (8)$$

This set of differential equations cannot be solved analytically

because the concentration of the active enzyme, [E], transiently and rapidly decreases in the presence of the carbamate inhibitor prior to slow restoration of E and hence of enzyme activity. However, values for *k*₅ and *k*₃/*K_C* can be calculated by numerical integrations of eqs 6–8 by the Runge–Kutta method (Carpenter, 1984), as detailed by Shin and Quinn (1992). Uncertainties in the parameters were estimated by assuming that the variation of χ^2 with respect to each parameter is independent of the values of the other parameters, in which case the following expression applies for the *j*th parameter *a_j* (Bevington, 1969):

$$\sigma_{a_j}^2 = \frac{2 \partial a_j}{\partial^2 \chi^2} \quad (9)$$

Figure 2 shows the fit constructed by fourth-order Runge–Kutta integration for transient inhibition of RCEase by 2-naphthyl-*N*-hexyl carbamate. The numerical simulation involves a grid search of combinations of the parameters *k*₅, *k*₃/*K_C*, and [E]_T, the analytical enzyme concentration, as described by Shin and Quinn (1992). For 2-naphthyl-*N*-butyl carbamate the intermediate F does not fully convert to the active enzyme E (cf. Scheme 1), and therefore an extra term is added to eq 8 for diversion of F to a non-reactivable form. Values for *k*₅ and *k*₃/*K_C* for reactions of various 2-naphthyl-*N*-alkyl carbamates generated by Runge–Kutta analysis are also tabulated in Table 2.

The inhibition phases for interaction of porcine CEase with all 18 carbamates in Table 1 were also characterized. The constants *k*₃ and *K_C*, determined for reactions in the presence and absence of NaTC, are tabulated in Table 3.

DISCUSSION

The numerous carbamylation reactions described herein possess several advantageous features for investigating molecular recognition by CEase of lipid substrates, and in particular of cholesteryl esters. First and most obvious is that, as the inhibitor is elaborated from phenyl to estronyl carbamate, the structural resemblance to cholesteryl esters increases considerably. Lipid substrates of CEase are so

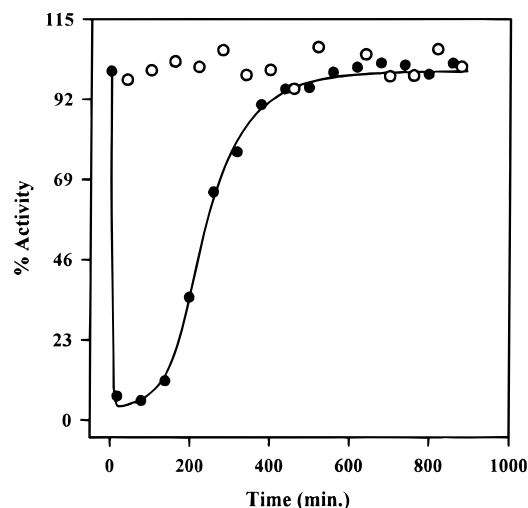


FIGURE 2: Stopped-time assay for transient inhibition of RCEase by 2-naphthyl-*N*-hexyl carbamate, **3**. The control, open circles, consisted of 64 nM RCE in 0.10 M sodium phosphate buffer, pH 7.00, that contained 0.16 M NaCl, 6 mM NaTC, and 2% acetonitrile (v/v). The inhibition reaction contained the same constituents plus 150 nM **3**. The incubation temperature was maintained at 25.0 ± 0.1 °C. At the indicated times, 40 μ L of either the control or inhibition reaction mixture was added to 2.00 mL of the aforementioned buffer and 40 μ L of 5.0 mM PNPB dissolved in HPLC-grade acetonitrile. RCEase activity was monitored at 400 nm on an HP8452A UV-visible diode array spectrophotometer. Initial rates were calculated for each assay by linear least-squares analysis. Percent activities were calculated by dividing the inhibited rates by the average control rate. The solid line represents the best fourth-order Runge-Kutta numerical simulation of the data; the parameters for this simulation are listed in Table 2. The value of $[E]_i$ obtained for this simulation is 6.14 ± 0.02 nM, or 96% of the expected value of 6.4 nM based on the mass of protein used in the experiment.

sparingly water soluble that they must be incorporated into supramolecular aggregates, such as micelles, microemulsions, or lipid films at the air-water interface (Smaby & Brockman, 1981a,b). A second advantage of the aryl carbamates is that they are of sufficient inhibitory potency that their interactions with CEase can be studied at low concentrations, at which the carbamates are probably monomeric species in homogeneous solution. Hence, the complications of interfacial catalysis, such as reversible binding of the enzyme to the lipid interface, are obviated. A third advantage is that the three stages of pseudo-substrate turnover of carbamates can be kinetically resolved. Hence, one can separate structure-activity effects on reversible binding of carbamates to the active site from the following serial carbamylation and decarbamylation steps. This kinetic resolution in turn allows an unprecedented resolution of bile salt activator effects on the three stages of the CEase mechanism to be effected. This is not possible with cholesteryl esters, since the effects of substrate structure on reversible binding of CEase to the lipid-water interface are not resolved from reversible binding of substrate to the active site and from the ensuing chemical events of catalytic turnover.

Structure-Activity Relationships for Reversible Binding. Linear free-energy relationships can be constructed from data in Table 2 for inhibition of RCEase. For the formation of the reversible complex EA (cf. Scheme 1), the energy of binding, both in the presence and absence of NaTC, is a linear function of the partial molecular volume of either the *N*-alkyl fragment (Figure 3A) or of the aryl fused-ring

Table 3: Kinetic Constants for Inhibition of PCEase by Aryl-*N*-alkyl Carbamates

compound	[NaTC] ^a (mM)	$10^2 k_3$ ^c (s ⁻¹)	K_c ^c (μ M)	$\ln(k_3/K_c)$
1	0 ^a	7 ± 1	15 ± 4	8.5 ± 0.2
	6.0 ^b	2.2 ± 0.3	1.9 ± 0.2	9.4 ± 0.2
2	0	2.0 ± 0.6	4 ± 1	8.5 ± 0.4
	6.0	0.9 ± 0.1	0.09 ± 0.02	11.5 ± 0.2
3	0	5.3 ± 0.6	2.7 ± 0.5	9.9 ± 0.2
	6.0	0.43 ± 0.05	0.029 ± 0.007	11.9 ± 0.3
4	0	6 ± 1	20 ± 6	8.0 ± 0.3
	6.0	3.4 ± 0.6	0.27 ± 0.08	11.8 ± 0.3
5	0	2.8 ± 0.2	12 ± 2	7.6 ± 0.2
	6.0	0.75 ± 0.01	0.08 ± 0.03	11.4 ± 0.4
7	0	9 ± 1	8 ± 2	9.3 ± 0.3
	6.0	6 ± 1	0.15 ± 0.04	12.9 ± 0.3
8	0	11 ± 2	9 ± 3	9.4 ± 0.4
	6.0	11 ± 3	0.04 ± 0.02	14.9 ± 0.7
9	0	ND	ND	4.42 ± 0.08
	6.0	0.53 ± 0.04	46 ± 7	4.8 ± 0.2
10	0	ND	ND	5.2 ± 0.1
	6.0	1.3 ± 0.2	60 ± 20	5.4 ± 0.4
11	0	3.7 ± 0.5	60 ± 20	6.4 ± 0.3
	6.0	4.9 ± 0.7	70 ± 20	6.6 ± 0.3
12	0	6 ± 1	130 ± 40	6.2 ± 0.4
	6.0	1.9 ± 0.2	20 ± 4	6.9 ± 0.2
13	0	ND	ND	5.5 ± 0.1
	6.0	0.42 ± 0.04	4 ± 1	7.0 ± 0.3
14	0	ND	ND	3.64 ± 0.05
	6.0	0.33 ± 0.03	18 ± 3	5.2 ± 0.2
15	0	8 ± 1	0.5 ± 0.1	12.0 ± 0.3
	6.0	4.7 ± 0.5	0.13 ± 0.02	12.8 ± 0.2
16	0	2.5 ± 0.4	36 ± 7	6.6 ± 0.3
	6.0	1.6 ± 0.2	6 ± 1	7.9 ± 0.2
17	0	6.0 ± 0.9	4 ± 1	9.6 ± 0.3
	6.0	5 ± 1	3 ± 1	9.7 ± 0.4
18	0	1.0 ± 0.2	3 ± 1	8.0 ± 0.3
	6.0	4.8 ± 0.4	1.6 ± 0.3	10.3 ± 0.2

^a Reactions were run at 25.0 ± 0.2 °C in 1.00 mL of 0.1 M sodium phosphate buffer, pH 7.06, that contained 0.10 M NaCl, 3 mM TX-100, 49 μ M PNPB, and 2% v/v acetonitrile. ND = not determined.

^b Same as footnote a, save that reactions contained 6 mM NaTC, 50 μ M PNPB, but no TX100. ^c Constants calculated by nonlinear least-squares fitting of k versus $[I]$ data to eq 3.

fragment (Figure 3B). These and similar free-energy relationships that are discussed below are described by an equation of the following form:

$$-\ln K_C = (\Delta G_0 - f\Delta\Delta G_f)/RT \quad (10)$$

This equation illustrates that the total binding free energy of the ligand (*i.e.*, $RT \ln K_C$) is a linear function of the fragment volume f , wherein ΔG_0 is the extrapolated binding energy at zero fragment volume and $\Delta\Delta G_f$ is the fragment volume-dependent change in the binding free energy. The magnitude of $\Delta\Delta G_f$ provides an experimental indication of the importance of hydrophobic interactions on ligand binding in the steroid and fatty acid binding loci of the CEase active site. Values of ΔG_0 and $\Delta\Delta G_f$ determined from the linear fits in Figure 3 are gathered in Table 4. Parameters from similar fits of data for inhibition of PCEase by aryl carbamates are also contained in the table.

Two interesting distinctions between the steroid binding site and the fatty acid binding site of RCEase can be gleaned from data in Table 4. The first is that the fatty acid binding site is considerably more hydrophobic than the steroid binding site, as evidenced by the larger $\Delta\Delta G_f$ values that accompany variation of the fragment size of the *N*-alkyl chain. The second is that NaTC has a more prominent effect

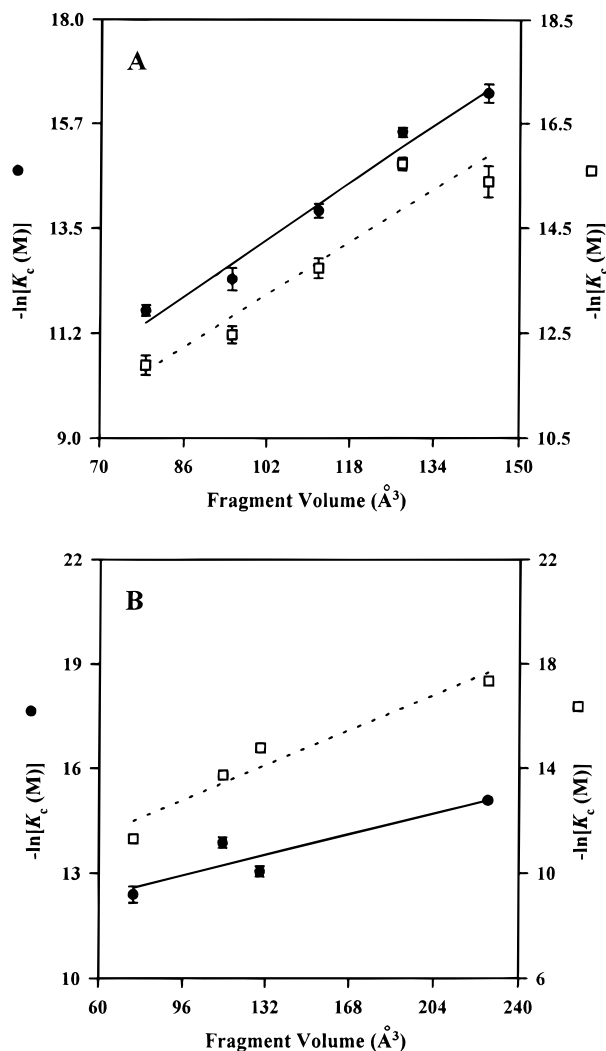


FIGURE 3: Linear free-energy relationships for formation of the reversible complex EA between RCEase and aryl carbamates. Circles and squares are for reactions in the absence and presence of 5.8 mM NaTC, respectively, and linear least-squares fits of the data to eq 10 are displayed. Reaction conditions are described in footnote *a* of Table 2. A. The fragment volume of the *N*-alkyl chain of 2-naphthyl-*N*-alkyl carbamates was varied. For reactions in the absence of NaTC (solid line), the parameters of the fit are $\Delta G_0 = 14 \pm 2 \text{ kJ mol}^{-1}$ and $\Delta \Delta G_f = -190 \pm 20 \text{ J mol}^{-1} \text{\AA}^3$. For reactions in the presence of NaTC (dashed line) the parameters of the fit are $\Delta G_0 = 17 \pm 4 \text{ kJ mol}^{-1}$ and $\Delta \Delta G_f = -160 \pm 30 \text{ J mol}^{-1} \text{\AA}^3$. B. The fragment volume of the aryl fused-ring system of aryl-*N*-hexyl carbamates was varied. For reactions in the absence of NaTC (solid line), the parameters of the fit are $\Delta G_0 = 28 \pm 2 \text{ kJ mol}^{-1}$ and $\Delta \Delta G_f = -40 \pm 10 \text{ J mol}^{-1} \text{\AA}^3$. For reactions in the presence of NaTC, the parameters of the fit are $\Delta G_0 = 23 \pm 3 \text{ kJ mol}^{-1}$ and $\Delta \Delta G_f = -90 \pm 20 \text{ J mol}^{-1} \text{\AA}^3$.

on molecular recognition in the steroid binding site than in the fatty acid binding site. For molecular recognition in the steroid binding site, increasing fragment volume leads to tighter binding. However, the $\Delta \Delta G_f$ value is significantly larger in the presence of 6 mM NaTC, a concentration above the critical micelle concentration of the bile salt, than in the absence of NaTC. In effect, binding of RCEase to NaTC micelles makes the steroid binding site look more hydrophobic, an appropriate evolutionary strategy for maximizing the catalytic power of the enzyme as a cholesteryl ester hydrolase. In contrast, $\Delta \Delta G_f$ values that arise from variation in the fatty acyl chain volume are statistically indistinguish-

Table 4: Binding Free-Energy Correlations for Aryl-*N*-alkyl Carbamate Inhibitors

varied fragment	enzyme	[NaTC] (mM)	ΔG_0^d (kJ mol $^{-1}$)	$\Delta \Delta G_f^d$ (J mol $^{-1} \text{\AA}^{-3}$)
<i>N</i> -alkyl chain	RCEase	0 ^a	14 ± 2	-190 ± 20
		5.82	17 ± 4	-160 ± 30
		6.00 ^c	31 ± 5	20 ± 50
aryl fused-ring system	PCEase	0	28 ± 2	-40 ± 10
		5.82	23 ± 3	-90 ± 20
		6.00	-27 ± 4	10 ± 30
			-29 ± 8	50 ± 50

^a See footnote *a* in Table 2. ^b See footnote *a* in Table 3. ^c See footnote *b* in Table 3. ^d Constants calculated by linear least-squares fitting of $-\ln K_c$ versus fragment volume to eq 10.

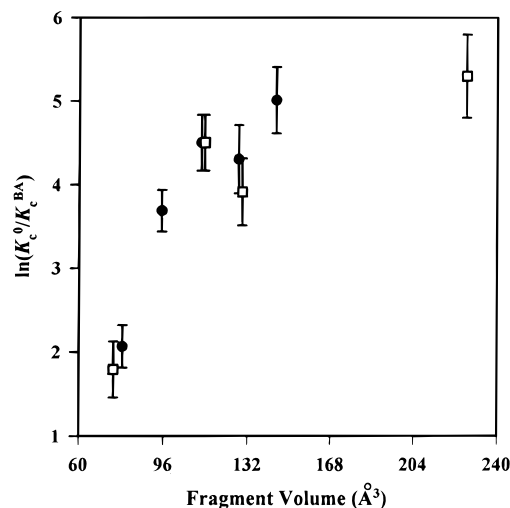


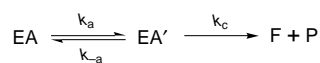
FIGURE 4: Nonlinear dependences of stimulation by NaTC of EA formation as a function of arylcarbamate fragment volume. Solid circles and open squares are respectively for reactions in which the fragment volumes of the *N*-alkyl chain of 2-naphthyl-*N*-alkyl carbamates and of the aryl fused-ring system of aryl-*N*-hexyl carbamates were varied. It is evident that both the steroid binding domain and the fatty acid bind site are similarly affected by NaTC. Reaction conditions are described in footnotes *a* and *b* of Table 3.

able; *i.e.*, binding of CEase to bile salt micelles has no effect on the hydrophobicity of the fatty acid binding site.

The effects of variation of carbamate structure are not nearly so systematic for PCEase as for RCEase. However, the enhancement brought about by NaTC of binding affinity in the reversible complex does increase systematically as the partial molecular volume of the *N*-alkyl chain or the aryl fused-ring system increases, as shown in Figure 4. It thus appears that bile salt activators conformationally modulate both the steroid and fatty acid binding sites on PCEase, in contrast to the lack of a bile salt effect on fatty acid recognition in RCEase.

Structure–Activity Relationships for Carbamylation. More complex nonlinear structure–activity relationships are observed for the chemical carbamylation step, monitored by rate constant k_3 . Figures 5A and 5B respectively show that $\ln k_3$ increases and decreases nonlinearly with increasing fragment size of the aryl fused-ring system and of the *N*-alkyl chain, with plateaus at high and low fragment size. Nonlinear structure–activity correlations such as these are consistent with a change in rate-determining step, and therefore suggest that the k_3 step consists itself of serial steps, as outlined in Scheme 2. In this situation the overall rate

Scheme 2



constant k_3 contains the rate constants of the serial steps:

$$k_3 = \frac{k_a k_c}{k_{-a} + k_c} = \frac{k_a k'_c}{k_a + k'_c} \quad (11)$$

In this equation $k'_c = k_a k_c / k_{-a}$. The rate constants k_a and k_{-a} are those for a reversible step, perhaps a conformational change of the enzyme or ligand, that precedes the chemical step (k_c) that produces the carbamylenzyme intermediate. If only the carbamylation step depends on the varied partial molecular volume of the ligand, then from transition-state theory (Glasstone *et al.*, 1941)

$$k'_c = \frac{k_B T}{h} e^{-\Delta G^*/RT} = \frac{k_B T}{h} e^{-(\Delta G_0^* + f\Delta\Delta G^*)/RT} \quad (12)$$

In this equation k_B , h , and T are Boltzmann's constant, Planck's constant, and the temperature in Kelvin, respectively. The free energy of activation, ΔG^* , is divided into parts that are independent, ΔG_0^* , and linearly dependent, $f\Delta\Delta G^*$, on fragment volume f . When eq 12 is substituted into eq 11 and the natural log transform is taken, a nonlinear free-energy relationship results:

$$\ln k_3 = \ln \left[\frac{k_a \frac{k_B T}{h} e^{-(\Delta G_0^* + f\Delta\Delta G^*)/RT}}{k_a + \frac{k_B T}{h} e^{-(\Delta G_0^* + f\Delta\Delta G^*)/RT}} \right] \quad (13)$$

The nonlinear fits in Figure 5 are to this equation, and provide $\Delta\Delta G^*$ values that are tabulated in Table 5. As the aryl fused-ring system more closely resembles a steroid, the fragment volume f increases and the free energy of activation progressively decreases because $\Delta\Delta G^*$ is negative, an indication of favorable hydrophobic interactions. As a consequence, the rate constant of the carbamylation step approaches a maximum. This is a reasonable observation from the teleological point of view. In that carbamylation is a model for the acylation stage of CEase catalysis, optimization of the carbamylation rate constant suggests that the acylation rate constant is similarly optimized. That is, the steroid binding site of RCEase has apparently evolved to take advantage of hydrophobic interactions with all four rings of the steroid fused-ring system, a strategy that optimizes the catalytic power of the enzyme as a cholesteryl ester hydrolase. How might hydrophobic interactions in the steroid binding site accelerate carbamylation or acylation of CEase? An hypothesis is that these interactions serve to position the carbonyl function adjacent to Ser194, which should lower the free energy of the nucleophilic attack component of the acylation or carbamylation step.

Addition of NaTC has a large effect on k_3 that is dependent on the size of the fragment that occupies the steroid binding site, as shown in Figure 5A. At low fragment size the bile salt effect is large (k_3 is increased ~ 100 -fold) but decreases to a less than 7-fold increase for the estronyl-*N*-hexyl carbamate. Consequently, in the presence of micellar NaTC the dependence of $\ln k_3$ on fragment volume is almost flat. These observations again support the idea that hydrophobic

interactions in the steroid binding site accelerate carbamylation or acylation. It has already been shown that, in the presence of NaTC, hydrophobic interactions in the reversible complex that precedes carbamylation are enhanced (cf. Structure–Activity Relationships for Reversible Binding). It is reasonable, then, that addition of bile salt will also accelerate carbamylation by increasing the hydrophobicity of the steroid binding site.

When the *N*-alkyl chain volume increases, $\ln k_3$ decreases in a nonlinear fashion that is opposite to that observed above when the steroid binding site was probed. The dependences of $\ln k_3$ on *N*-alkyl chain volume are well described by fitting to eq 13, as shown in Figure 5B; the corresponding parameters are gathered in Table 5. In this case, increasing the hydrophobicity of the substituent decreases k_3 by decreasing the carbamylation rate constant k_c . A probable cause for the systematic decrease in k_c is that, as the length of the *N*-alkyl chain increases, the torsional and other vibrational degrees of freedom of the chain increase, and consequently the entropy of the *N*-alkyl chain increases. If the conformational options available to the *N*-alkyl chain are more restricted in the carbamylation transition state than in the reversible complex that precedes it, then increasing the chain length will produce an increasingly negative ΔS^* . This in turn will increase ΔG^* progressively as the length of the *N*-alkyl chain increases, as indicated by the positive $\Delta\Delta G^*$ values in Table 5.

The addition of the bile salt activator NaTC shifts the *N*-alkyl chain dependence upward but does not affect its shape, as shown in Figure 5B. Therefore, NaTC increases k_3 in a manner that is independent of *N*-alkyl chain length, an indication that bile salt does not modulate the fatty acid binding site of RCEase. Rather, the role of bile salt is to modulate the steroid binding site, in agreement with observations discussed above (cf. Structure–Activity Relationships for Reversible Binding) that NaTC increases the hydrophobicity of the steroid binding site but leaves the hydrophobicity of the fatty acid binding site unaltered.

Structure–Activity Effects for Second-Order Inhibition. PCEase and RCEase also show a common behavior when the second-order inhibition rate constant is plotted, as $\ln k_3/K_C$, against the partial molecular volume of the *N*-alkyl chain. These plots, shown in Figure 6, indicate that for both enzymes there is a particular *N*-alkyl chain length at which activity is a maximum, both in the presence and absence of NaTC micelles. For inhibition of PCEase by both 2-naphthyl and *p*-acetamidophenyl *N*-alkyl carbamates, activity reaches a maximum in the absence of NaTC at a chain length of six carbons, equivalent to an eight carbon fatty acid (cf. Figure 6, A and B). When NaTC micelles are added, $\ln k_3/K_C$ is increased in a chain length dependent manner, plotted as bar graphs in Figure 6D, and the maxima are shifted to longer alkyl chains. Moreover, the upward shift effected by bile salt in the *N*-alkyl chain length dependence is greater for 2-naphthyl than for *p*-acetamidophenyl carbamates. Hence, bile salt activators conformationally modulate both the steroid and fatty acid binding sites of PCEase, in contrast to the lack of modulation of the fatty acid binding site for RCEase. The plots in Figure 6C for RCEase underscore this species difference. Both in the presence and absence of NaTC, there are maxima at a chain length of seven carbons, and the stimulation due to bile salt is chain-length independent (Figure 6D). Again the upward shift in the dependence

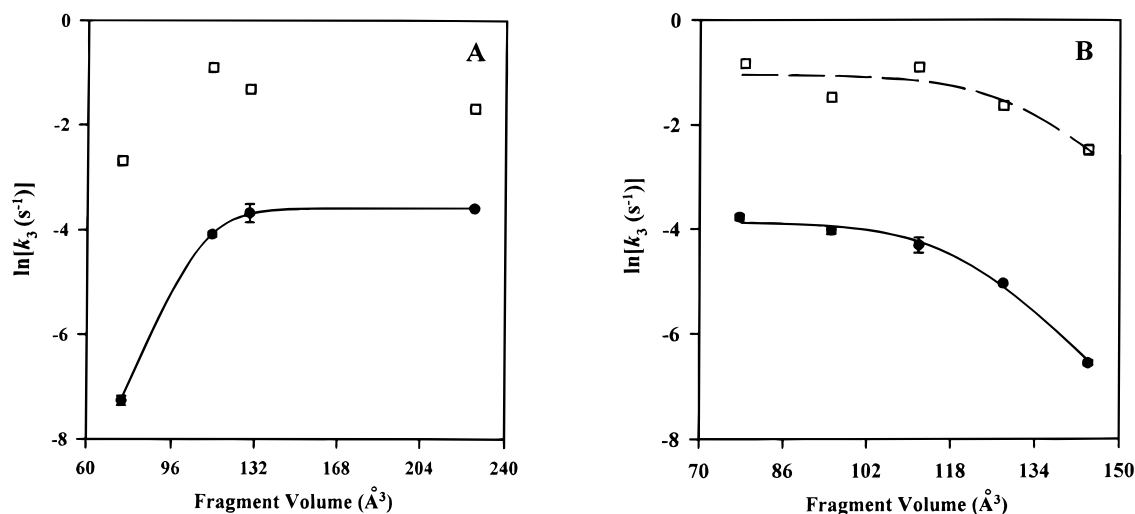


FIGURE 5: Nonlinear dependence of $\ln k_3$ on fragment volume for inhibition of RCEase by aryl-*N*-alkyl carbamates. Circles and squares are for reactions in the absence and presence of 5.8 mM NaTC, respectively. Reaction conditions are described in footnote a of Table 2. A. The fragment volume of the aryl fused-ring system of aryl-*N*-hexyl carbamates was varied. The solid line is a nonlinear least-squares fit to eq 13, and the parameters of the fit are $k_a = (2.76 \pm 0.05) \times 10^{-2} \text{ s}^{-1}$, $\Delta G_0^* = 110.5 \pm 0.4 \text{ kJ mol}^{-1}$, and $\Delta \Delta G^* = -262 \pm 5 \text{ J mol}^{-1} \text{ Å}^3$. B. The fragment volume of the *N*-alkyl chain of 2-naphthyl-*N*-alkyl carbamates was varied. Solid lines are nonlinear least squares fits to eq 13. For reactions in the absence of NaTC, the parameters of the fit are $k_a = (2.0 \pm 0.2) \times 10^{-2} \text{ s}^{-1}$, $\Delta G_0^* = 52 \pm 4 \text{ kJ mol}^{-1}$, and $\Delta \Delta G^* = 260 \pm 30 \text{ J mol}^{-1} \text{ Å}^3$. For reactions in the presence of NaTC, the parameters of the fit are $k_a = 0.40 \pm 0.01 \text{ s}^{-1}$, $\Delta G_0^* = 43 \pm 20 \text{ kJ mol}^{-1}$, and $\Delta \Delta G^* = 300 \pm 200 \text{ J mol}^{-1} \text{ Å}^3$.

Table 5: Free-Energy Correlations for Carbamylation of Cholesterol Esterase by Aryl-*N*-alkyl Carbamate Inhibitors

varied fragment	enzyme	[NaTC] (mM)	$10^2 k_a$ (s ⁻¹)	ΔG_0^* (kJ mol ⁻¹)	$\Delta \Delta G^*$ (J mol ⁻¹ Å ⁻³)
<i>N</i> -alkyl chain	RCEase ^a	0 ^b	2.0 ± 0.2	52 ± 4	260 ± 30
		5.82	40 ± 1	43 ± 20	300 ± 200
	PCEase ^c	0 ^d	NA	7 ± 3	-10 ± 30
		6.00 ^e	NA	10 ± 5	-10 ± 50
aryl fused-ring system	RCEase	0	2.76 ± 0.05	110.5 ± 0.4	-262 ± 5
		5.82	NA	NA	NA
	PCEase	0	NA	10 ± 1	-20 ± 10
		6.00	NA	14 ± 4	-40 ± 30

^a Values for ΔG_0^* and $\Delta \Delta G^*$ were calculated by nonlinear least-squares fitting of $\ln k_3$ versus fragment volume to eq 13. ^b See footnote a in Table 2. ^c Values for ΔG_0^* and $\Delta \Delta G^*$ were calculated by linear least-squares fitting of $\ln k_3$ versus fragment volume to the natural log transformation of eq 12 in which k_3 has been substituted for k'_3 . ^d See footnote a in Table 3. ^e See footnote b in Table 3.

brought about by bile salt must arise from conformational modulation of the steroid binding site. Maxima similar to those reported herein have been reported for the rate of PCEase-catalyzed hydrolysis of mixed micellar fatty acyl *p*-nitrophenyl esters (Sutton *et al.*, 1990a) and for the affinity of alkylboronic acid inhibitors of PCEase (Sutton *et al.*, 1990b).

The electronic nature of the carbamylation transition state was probed by measuring k_3/K_C for *p*-substituted phenyl-*N*-hexyl carbamates, compounds 11 and 15–18 in Table 1; the corresponding data are in Table 3. Hammett plots, constructed according to eq 14, are shown in Figure 7 (Hansch

$$\log \frac{k_3}{K_C} = \rho \sigma_p^- + C \quad (14)$$

& Leo, 1979; Hansch *et al.*, 1991). The slopes of the Hammett plots are $\rho = 1.8 \pm 0.4$ in the absence of NaTC and $\rho = 2.0 \pm 0.2$ in the presence of 6 mM NaTC. Similar results of Hammett analysis have been reported for inhibition of bovine CEase by aryl-*N*-butyl carbamates (Lin & Lai,

1995). That the ρ values are greater than one indicates that the carbamylation transition state is more sensitive to aryl substituents than are the reference processes, the ionizations of *p*-substituted phenols and anilinium ions (Leffler & Grunwald, 1963), that are used to define the substituent constants, σ_p^- . In phenol ionization the phenolic oxygen acquires a full negative charge. Therefore, the Hammett analysis described herein necessitates that departure of the leaving group is the rate-determining step, and that in the carbamylation transition state the bond to the phenolic leaving group must be completely broken and the phenolic oxygen must be carrying a unit negative charge. Why are the slopes of the Hammett plots greater than 1, when the charges on the phenolic oxygen are -1 both upon phenol ionization, the reference process, and in the carbamylation transition state? This likely reflects the fact that the phenolate anion in the carbamylation transition state is made in a relatively hydrophobic active site, whereas upon phenol ionization the charge on the phenolate anion is partially masked by H-bonding with water.

Structure–Activity Relationships for Decarbamylation. Linear free-energy relationships are observed both in the presence and absence of NaTC for turnover of the carbamyl-RCEase intermediate, k_5 , as a function of increasing partial molecular volume of the *N*-alkyl chain, as shown in Figure 8. These relationships can be interpreted by writing an equation identical in form to eq 12, albeit with k_5 as the dependent variable and expressed as the natural log transform:

$$\ln k_5 = \ln \frac{k_B T}{h} - \frac{\Delta G_0^*}{RT} - \frac{f \Delta \Delta G^*}{RT} \quad (15)$$

Least-squares analysis according to eq 15 of the data plotted in Figure 8 gives $\Delta \Delta G^*$ values of 32 ± 4 and $-30 \pm 10 \text{ J mol}^{-1} \text{ Å}^{-3}$ for reactions in the absence and presence of bile salt, respectively. The chain length dependent increasing stimulation effected by NaTC suggests that bile salts increase

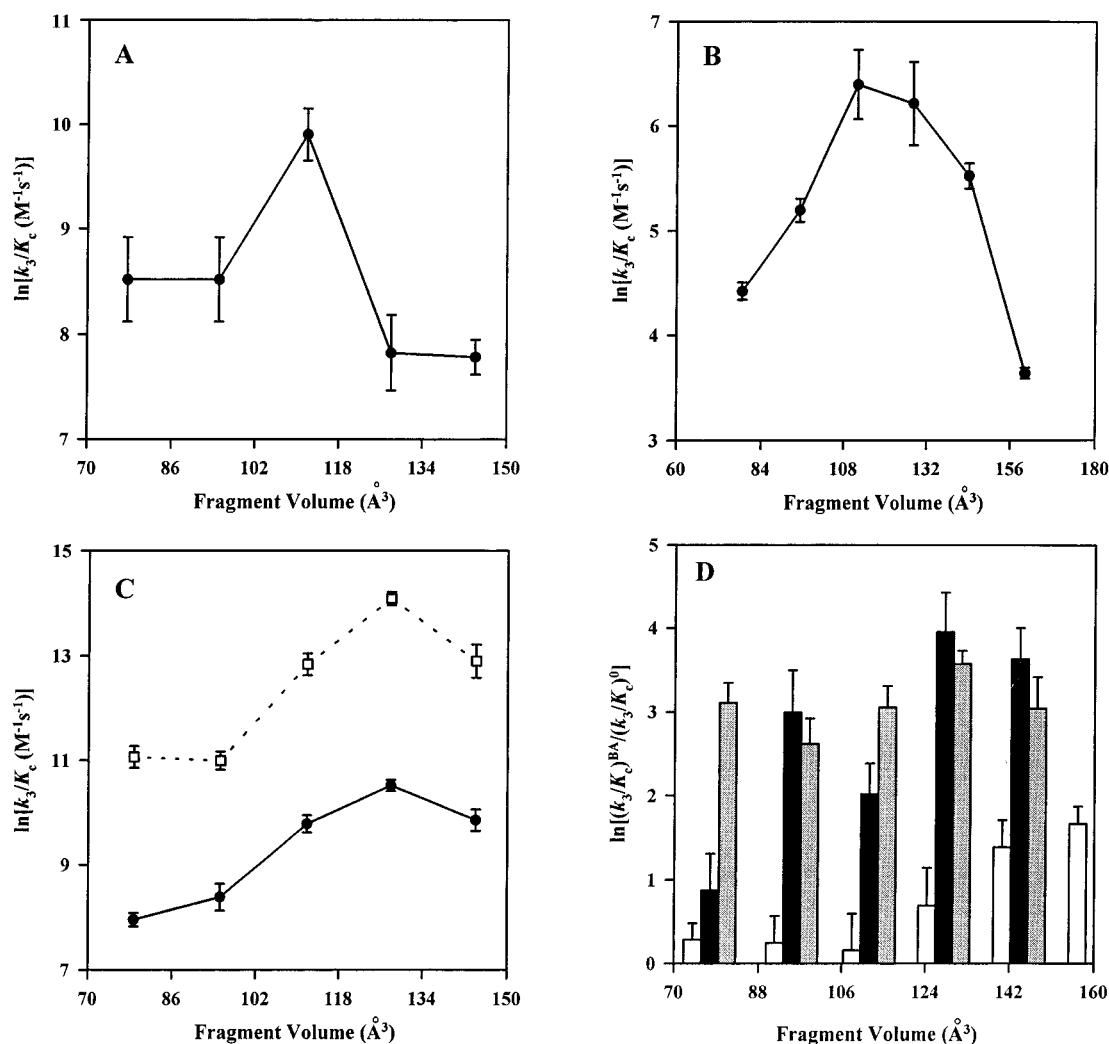


FIGURE 6: Dependence of $\ln(k_3/K_C)$ on *N*-alkyl chain length for inhibition of CEase by aryl-*N*-alkyl carbamates. A, B. The fragment volumes of the *N*-alkyl chains of 2-naphthyl-*N*-alkyl (panel A) and *p*-acetamidophenyl-*N*-alkyl (panel B) carbamates were varied for inhibitions of PCEase. Reaction conditions are described in footnote a of Table 3. C. Dependence of $\ln(k_3/K_C)$ on fragment volume of the *N*-alkyl chain for inhibition of RCEase by 2-naphthyl-*N*-alkyl carbamates. Filled circles and open squares are for reactions in the absence and presence of 6 mM NaTC, respectively. Reaction conditions are described in footnote a of Table 2. D. Bar graph of the natural log of the stimulation of k_3/K_C effected by NaTC, as a function of *N*-alkyl chain volume, for inhibition of CEase. Open bars are for inhibition of PCEase by *p*-acetamidophenyl-*N*-alkyl carbamates. Black and gray bars are for inhibitions of PCEase and RCEase, respectively, by 2-naphthyl-*N*-alkyl carbamates. Reaction conditions for the PCEase reactions are described in footnotes a and b of Table 3, and for RCEase in footnote a of Table 2.

the hydrophobic sensitivity of the fatty acid binding site in the decarbamylation transition state, and by implication in the deacylation transition state for turnover of lipid substrates. Therefore, bile salts effect each of the phases of CEase catalysis in a manner that increases the catalytic power of the enzyme.

Conclusions. Various structure–activity relationships are described herein for inhibition of mammalian CEases by aryl carbamates. Not surprisingly, these SARs indicate that CEase utilizes hydrophobic interactions in the steroid and fatty acyl binding sites for molecular recognition. Of some surprise, however, is the magnitude of the interactions. For example, the $\Delta\Delta G_f$ value in the absence of NaTC in Table 4 for reversible binding in the fatty acid site of RCEase, $-190 \pm 20 \text{ J mol}^{-1} \text{ \AA}^{-3}$, can also be expressed as $-3100 \pm 300 \text{ J mol}^{-1}$ per methylene. This value is comparable to the free energy increment, -3450 J mol^{-1} per methylene, for transfer of amphiphilic compounds from water to hydrocarbon phases (Tanford, 1980). Moreover, the log *P* value, which measures the effect of a substituent on phase transfer from water to

n-octanol (Hansch & Leo, 1979), of a methylene unit corresponds to a free energy increment of -3760 J mol^{-1} . Therefore, the fatty acid binding site is comparable in hydrophobicity to a neat hydrocarbon solvent.

The $\Delta\Delta G_f$ values for reversible interaction in the steroid binding site of RCEase are considerably less negative than those for the fatty acid binding site, an indication that of the two loci the steroid binding site utilizes hydrophobic interactions less extensively. Modeling of the structure of RCEase (Feaster *et al.*, 1996) reveals putative steroid and fatty acid binding sites for molecular recognition of cholesteryl esters that possess the hydrophobic characteristics indicated by the $\Delta\Delta G_f$ values in Table 4. The side chains that line the proximal portion of the fatty acid binding site, that portion that can interact with a carbamyl function of up to eight carbons in length, are a mix of hydrophobic and polar residues: Ile281, Val282, His283, Phe324, Ala325, Glu388, Leu392. Amino acid side chains that line the steroid binding site are almost exclusively hydrophobic: Pro99, Met101,

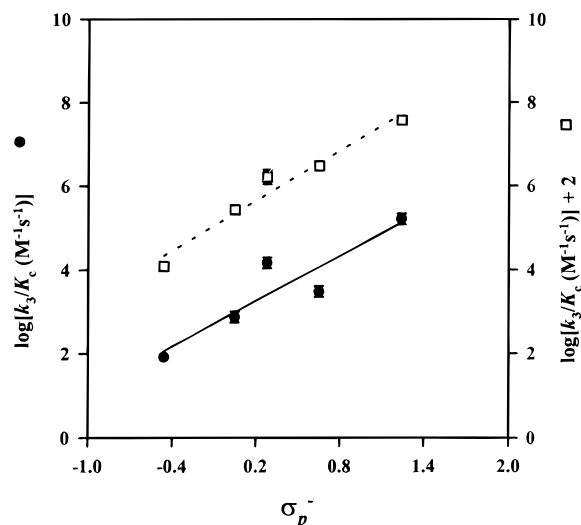


FIGURE 7: Hammett plots for the second-order rate constant of inhibition of PCEase by *p*-substituted phenyl-*N*-hexyl carbamates. Filled circles and open squares are for reactions in the absence and presence of 6 mM NaTC, respectively. Straight lines are linear least-squares fits to eq 14 and give $\rho = 1.8 \pm 0.4$ (solid line) and $\rho = 2.0 \pm 0.2$ (dashed line) for reactions in the absence and presence of NaTC, respectively. Reaction conditions are described in footnotes *a* and *b* of Table 3.

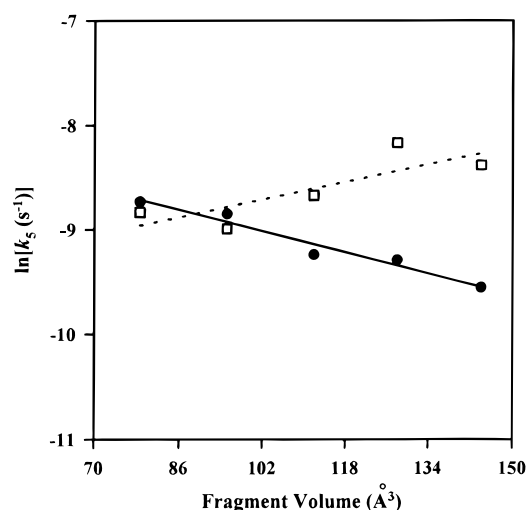


FIGURE 8: Linear free-energy correlations between the rate constant for decarbamylation of the carbamyl-RCEase intermediate, k_5 , and the partial molecular volume of the *N*-alkyl chain of the carbamate. Lines were generated by linear least-squares fitting to eq 15 of data for reactions in the absence of NaTC (circles, solid line) and in the presence of 5.8 mM NaTC (squares, dashed line). The parameters of the fit for reactions in the absence of NaTC are $\Delta G_0^* = -10.4 \pm 0.4 \text{ kJ mol}^{-1}$ and $\Delta\Delta G^* = 32 \pm 4 \text{ J mol}^{-1} \text{ \AA}^{-3}$, and those for reaction in the presence of NaTC are $\Delta G_0^* = -5 \pm 1 \text{ kJ mol}^{-1}$ and $\Delta\Delta G^* = -30 \pm 10 \text{ J mol}^{-1} \text{ \AA}^{-3}$. Experimental conditions are described in the legend of Figure 2, save that bile salt is excluded for reactions in the absence of NaTC.

Trp103, Leu124, Tyr125, Val136, Val138, Phe191, Leu439, Phe443, Ala472. Therefore, it is somewhat surprising that the $\Delta\Delta G_f$ value for the fatty acid binding site is consistent with greater importance of hydrophobic interactions than for the steroid binding site. The hydrophobic character of the steroid binding site is utilized more extensively to stabilize the carbamylation transition state, rather than the reversible complex that precedes it, an assertion that is supported by the $\Delta\Delta G^*$ value of $-262 \text{ J mol}^{-1} \text{ \AA}^{-3}$ that arises from analysis of the nonlinear dependence of $\ln k_3$ on the size of the aryl fused-ring system in Figure 5A.

Resolution of the mechanism of turnover of pseudo-substrate aryl carbamates into successive active site binding, carbamylation and decarbamylation steps allows one to define in some detail the role of bile salt activators. Usually, NaTC enhanced the hydrophobic nature of molecular recognition by CEase. NaTC increases the contribution of hydrophobic effects to steroid binding by both RCEase and PCEase. NaTC enhances the hydrophobic selectivity of the fatty acid binding site of PCEase in the carbamylation transition state and of RCEase in the decarbamylation transition state. The fact that NaTC selectively modulates the steroid binding domain for RCEase is consistent with the observation that bile salts modulate the stereoselectivity of the hydrolysis of α -tocopheryl acetates by porcine and bovine CEase (Zahalka *et al.*, 1991).

It is instructive to compare bile salt effects reported herein with those reported by Wang (1991) for human milk bile salt activated lipase (human CEase) catalyzed hydrolysis of short-chain fatty acyl *p*-nitrophenyl esters. He measured the effect of NaTC on the Michaelis-Menten kinetic parameters k_{cat} and K_m . He correctly ascribed the bile salt effect on k_{cat} to effects on the chemical step(s) of catalysis. However, CEase catalysis proceeds by an acylenzyme mechanism (Stout *et al.*, 1985; Lombardo & Guy, 1981), as outlined in Scheme 1, for which k_{cat} is given by the following equation:

$$k_{\text{cat}} = \frac{k_3 k_5}{k_3 + k_5} \quad (16)$$

Therefore, Wang's analysis did not resolve bile salt effects on acylation and deacylation. Lombardo & Guy (1981) trapped the acylenzyme intermediate in human CEase-catalyzed hydrolysis of *p*-nitrophenyl acetate with alcohols, and therefore the rate-limiting step monitored by k_{cat} is deacylation, *i.e.*, $k_{\text{cat}} = k_5$. Moreover, Wang ascribed bile salt effects on K_m to effects on reversible substrate binding. This attribution is certainly not justified, since K_m for the acylenzyme mechanism of Scheme 1 is

$$K_m = \frac{k_2 + k_3}{k_1} \frac{k_5}{k_3 + k_5} \quad (17)$$

For the case of rate-determining deacylation, as demonstrated by Lombardo and Guy (1981), the second term in K_m reduces to k_5/k_3 . Therefore, bile salt effects on K_m do not uniquely resolve effects on k_2/k_1 , *i.e.*, reversible substrate binding. The structure-activity relationships described herein neatly avoid the complications and vagaries of the kinetically unresolved acylenzyme mechanism.

CEase is a potential target for the development of hypocholesterolemic agents, particularly in light of the recently reported correlations between plasma CEase activities and total plasma cholesterol or LDL concentrations (Brodt-Eppley *et al.*, 1995). The structure-activity relationships reported herein suggest the required features of a maximally potent CEase inhibitor. One is that the steroid binding site be fully occupied; truncated structures, such as mononuclear aromatics, are much less potent inhibitors. A second feature is a good leaving group, as supported by the Hammett plots of Figure 7; an inhibitor that possesses a secondary alcohol rather than a phenol leaving group is predicted to be of considerably reduced potency. A third feature is a fatty acyl chain of intermediate length; carbamyl

chains of six or seven carbons are optimal. Going beyond this length will seriously impair inhibitor potency, a trend that is paralleled by structure–activity effects as a function of acyl chain length for human CEase-catalyzed hydrolysis of monoacylglycerols and short acyl chain *p*-nitrophenyl esters (Wang, 1991) and by PCEase-catalyzed hydrolysis of fatty acyl *p*-nitrophenyl esters (Sutton *et al.*, 1990a).

REFERENCES

- Abouakil, N., Rogalska, E., & Lombardo, D. (1989) *Biochim. Biophys. Acta* 1002, 225–230.
- Baba, T., Downs, D., Jackson, K., Tang, J., & Wang, C.-S. (1991) *Biochemistry* 30, 500–510.
- Bevington, P. R. (1969) in *Data Reduction and Error Analysis for the Physical Sciences*, pp 242–245, McGraw-Hill, New York.
- Brockerhoff, H., & Jensen, R. G. (1974) in *Lipolytic Enzymes*, pp 176–193, Academic Press, New York.
- Brodth-Eppley, J., White, P., Jenkins, S., & Hui, D. Y. (1995) *Biochim. Biophys. Acta* 1272, 69–72.
- Carpenter, B. K. (1984) in *Determination of Organic Reaction Mechanisms*, pp 76–82, John Wiley & Sons, New York.
- Cygler, M., Schrag, J. D., Sussman, J. L., Harel, M., Silman, I., Gentry M. K., & Doctor, B. P. (1993) *Protein Sci.* 2, 366–382.
- DiPersio, L. P., & Hui, D. Y. (1993) *J. Biol. Chem.* 268, 300–304.
- DiPersio, L. P., Fontaine, R. N., & Hui, D. Y. (1990) *J. Biol. Chem.* 265, 16801–16806.
- DiPersio, L. P., Fontaine, R. N., & Hui, D. Y. (1991) *J. Biol. Chem.* 266, 4033–4036.
- Feaster, S. R., Quinn, D. M., & Barnett, B. L. (1996) *Protein Sci.* (in press).
- Fredrikzon, B., Hernell, O., Bläckberg, L., & Olivercrona, T. (1978) *Pediatr. Res.* 12, 1048–1052.
- Gallo, L. L., Newbill, T., Hyun, J., Vahouny, G. V., & Treadwell, C. R. (1977) *Proc. Soc. Exp. Biol. Med.* 156, 277–281.
- Glasstone, S., Laidler, K. J., & Eyring, H. (1941) in *The Theory of Rate Processes*, McGraw-Hill, New York.
- Hansch, C., & Leo, A. (1979) in *Substituent Constants for Correlation Analysis in Chemistry and Biology*, John Wiley & Sons, New York.
- Hansch, C., Leo, A., & Taft, R. W. (1991) *Chem. Rev.* 91, 165–195.
- Hui, D. Y., Hayakawa K., & Oizumi J. (1993) *Biochem. J.* 291, 65–69.
- Kazlauskas, R. J. (1989) *J. Am. Chem. Soc.* 111, 4953–4959.
- Kraut, J. (1977) *Annu. Rev. Biochem.* 46, 331–358.
- Kritchevsky, D., & Kothari, H. V. (1978) *Adv. Lipid Res.* 16, 221–226.
- Leffler, J. E., & Grunwald, E. (1963) in *Rates and Equilibria of Organic Reactions*, pp 211–214, John Wiley & Sons, New York.
- Lin, G., & Lai, C.-Y. (1995) *Tetrahedron Lett.* 36, 6117–6120.
- Lombardo, D., & Guy, O. (1981) *Biochim. Biophys. Acta* 657, 425–437.
- Ollis, D. L., Cheah, E., Cygler, M., Dijkstra, B., Frolow, F., Fraken, S. M., Harel, M., Remington, S. J., Silman, I., Schrag, J., Sussman, J., Verschueren, K. H. G., & Goldman, A. (1992) *Protein Eng.* 5, 197–211.
- Rudd, E. A., & Brockman, H. L. (1984) in *Lipases* (Borgström, B., & Brockman, H. L., Eds.) pp 185–204, Elsevier, Amsterdam.
- Shin, H.-C., & Quinn, D. M. (1992) *Biochemistry* 31, 811–818.
- Smaby, J. M., & Brockman, H. L. (1981a) *Biochemistry* 20, 718–723.
- Smaby, J. M., & Brockman, H. L. (1981b) *Biochemistry* 20, 724–730.
- Stout, J. S., Sutton, L. D., & Quinn, D. M. (1985) *Biochim. Biophys. Acta* 837, 6–12.
- Sutton, L. D., Stout, J. S., & Quinn, D. M. (1990a) *J. Am. Chem. Soc.* 112, 8398–8403.
- Sutton, L. D., Lantz, J. L., Eibes, T., & Quinn, D. M. (1990b) *Biochim. Biophys. Acta* 1041, 79–82.
- Tanford, C. (1980) in *The Hydrophobic Effect: Formation of Micelles and Biological Membranes*, pp 14–28, John Wiley & Sons, New York.
- Wang, C.-S. (1991) *Biochem. J.* 279, 297–302.
- Wentworth, W. E. (1965) *J. Chem. Ed.* 42, 96–103.
- Zahalka, H. A., Dutton, P. J., O'Doherty, B., Smart, T. A.-M., Phipps, J., Foster, D. O., Burton, G. W., & Ingold, K. U. (1991) *J. Am. Chem. Soc.* 113, 2797–2799.

BI961677V